Tri Dasa Mega Vol. 27 No. 1 (2025) 29-38

Journal of Nuclear Reactor Technology

Tri Dasa Mega

Journal homepage: https://ejournal.brin.go.id/tridam

Optimizing Boron Dose for Cervical Cancer Therapy Using BNCT and PHITS Simulations

Laili Rochimah[1], Subur Pramono[1], Beta Nur Pratiwi[1], Yohannes Sardjono[2], Gede Sutresna Wijaya[2], Isman Mulyadi Triatmoko[2], Nunung Nuraeni[2], Heru Prasetio[2], Nur Rahmah Hidayati[2], Syarifatul Ulya[2], Zuhdi Ismail[2]

[1]*Department of Physics, Faculty of Science, Sultan Maulana Hasanuddin State Islamic University, 42171, Banten, Indonesia*
[2]*Research Center for Safety, Metrology and Nuclear Quality Technology, Research Organization for Nuclear Energy, The National Research and Innovation Agency, Tangerang Selatan, Indonesia*

ARTICLE INFO

Article history:

Received: December 3, 2024
Received in revised form: January 15, 2025
Accepted: January 20, 2025

Keywords:

BNCT
Dosimetry
Cervical
PHITS

A B S T R A C T

Cervical cancer, with approximately 569.000 new cases annually, ranks as the fourth most prevalent malignancy among women worldwide. This high incidence rate significantly contributes to its position as one of the leading causes of cancer-related mortality worldwide. *Boron Neutron Capture Therapy* (BNCT), a form of radiotherapy based on the neutron capture principle, utilizes boron-10 as a targeted agent for destroying cancer cells. In this study, the geometry of cervical cancer tissue and surrounding healthy organs was simulated under neutron irradiation, using boron concentrations of 100, 120, and 140 μg/g from the *left-lateral* and *posterior-anterior* directions. This study aimed to determine the optimal boron concentration and irradiation time for effective eradication of stage IIIA cervical cancer while minimizing side effects. The *Particle and Heavy Ion Transport Code System* (PHITS) was employed to model particle transport and dose distribution. Simulation results indicate that the total dose rate required for tumor eradiction in the 8.68×10^{-2} Gy/s Gross Tumor Volume (GTV) is achieved at a boron concentration of 140 μg/g, with minimal impact on surrounding tissues, and an optimal irradiation time of 18 minutes 22 seconds from the *left-lateral* direction.

1. INTRODUCTION*

Cancer is caused by the uncontrolled development of abnormal cells within the body's tissue [1]. According to GLOBOCAN 2022, cervical cancer is among the leading causes of cancer-related deaths worldwide. Cervical cancer ranks eighth globally, with 662.301 reported cases and 348.874 deaths, placing it ninth in cancer mortality worldwide [1]. Cervical cancer develops in the cervix, specifically affecting its outer epithelial layer [2]. Globally, cervical cancer poses a significant threat to women's health [1]. The etiology of cervical cancer is multifactorial, with *human papillomavirus* (HPV) infection being the most common cause [1, 3]. HPV infection, alongside risk factors such as smoking and multiple sexual partners, is strongly associated with cervical cancer [1]. Cervical cancer can be treated using various therapeutic approaches [4].

*Corresponding author
Email:lailir777@gmail.com
DOI:10.55981/tdm.2025.7150

The selection of an appropriate cancer therapy is crucial for patient survival, with minimal side effects being a key consideration [4]. *Boron Neutron Capture Therapy* (BNCT) is an innovative treatment approach that minimizes side effects by specifically targeting cancer cells for destruction [4, 5]. The principle of BNCT, as described in Eq.1, involves the interaction between boron-10 and thermal neutrons, producing boron-11. Boron-11 subsequently decays via two pathways: 6.1% produce alpha particles with energy 2.79 MeV, and 93.9% produce lithium nuclei releasing 2.31 MeV [6].

$$[^{10}_{5}B] + [^{1}_{0}n] \rightarrow [^{11}_{5}B]^*$$

$$(1{,}78\ MeV) + (1{,}01\ MeV)$$

$$[^{11}_{5}B]^* \rightarrow [^{4}_{2}He] + [^{7}_{3}Li] + 2{,}79\ MeV\ (6.1\%)$$

$$(1{,}78\ MeV) + (0{,}84\ MeV)$$

$$[^{11}_{5}B]^* \rightarrow [^{4}_{2}He] + [^{7}_{3}Li]^* + 2{,}31\ MeV\ (93.9\%)$$

$$\downarrow$$

$$[^{7}_{3}Li] + \gamma\ 0{,}48\ MeV \qquad (1)$$

The foundation of BNCT lies in nuclear processes, specifically the interaction between thermal neutrons and the isotope boron-10, resulting in the formation of boron-11, which then decays into α-particles and lithium nuclei, as shown in Figure 1 [7]. In BNCT, boron is used to calculate the radiation dose absorbed by cancerous and surrounding healthy tissue [4].

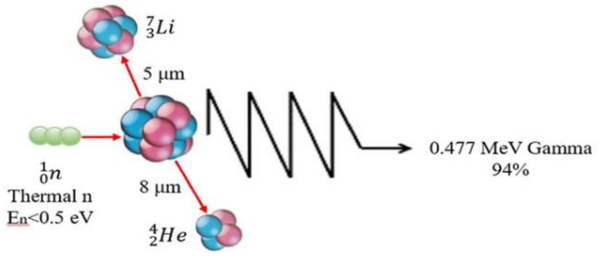

Figure 1. BNCT reaction scheme in cells [8]

Boron-10 is used because it has a high thermal neutron absorption cross section, as shown in Table 1 [9]. This neutron capture reaction produces a high *Linear Energy Transfer* (LET) KeV ≈150 KeV/µm for $\alpha -$ particles and talmost equal to≈175 KeV/µm for lithium nuclei [10]. A precise LET measurement is critical for administering the appropriate dose to the patient, ensuring both efficacy and safety in treatment protocols [11]. This reaction produces a high LET capable of damaging cancer tissue at the cellular level, with alpha particles and lithium nuclei having a short range of 5-8 µm, approximately equivalent to the diameter of a single cell [10, 11]. This localized energy deposition minimizes radiation damage to surrounding healthy cells [12].

Table 1. Comparison of neutron capture elements [9]

No	Element	Cross Section ($\boldsymbol{\sigma}$)
1	Nitrogen	13.481
2	Hydrogen	32.945
3	Boron-10	3835

Very low-energy neutron capture cross sections are important for research and practical uses in nuclear science [13]. A cross-section quantifies the probability of a reaction occurring with an atomic nucleus. It can be conceptualized as an effective target area representing this probability. If a particle hits a circular area of this size, placed in the right direction towards the target particle, then a reaction can happen. The larger this area, the greater the chance that a reaction will occur [14].

Dose calculations for large amounts of radiation energy deposited in biological tissues cannot be measured directly. This comprehensive dose calculation may employ software such as the *Particle and Heavy Ion Transport Code System* (PHITS). PHITS simulations are essential because the software can model a wide range of particles, including neutrons, protons, heavy ions, photons, and electrons. This versatility makes PHITS a critical tool for analyzing complex interactions in various applications [15, 16]. Dosage must be carefully assessed when analyzing neutrons- boron interactions. Higher boron concentrations shorten the required irradiation time, selectively destroying cancer cells while sparing healthy tissue [3, 4]. Irradiation duration is determined by dividing the minimum required therapeutic dose by the total dose rate [6]. The concentration of boron needs to be optimized to avoid toxicity; therefore, this study evaluated concentrations of 100, 120, and 140 µg/g, with irradiation applied from both *left-lateral* and *posterior-anterior* directions [5]. The dosage range was selected based on the minimum concentration required to effectively target and eliminate cancer cells, set at 15 µg/g. In contrast, the maximum permissible concentration of boron is established at 150 µg/g [17]. This investigation examined the impact of different boron concentrations on the kinetics of radiation-induced carcinogenesis. According to Agestha M. 2023, at a concentration of 80 µg/g, the associated cancer dose rate measured 0.0167 Gy/s. In contrast, an increased concentration resulted in a dose rate of 0.0283 Gy/s. The findings suggest that an increase in boron concentration

corresponds with a rise in the radiation dose rate, indicating that prolonged exposure may lead to more significant effects. For subsequent analyses, the researchers selected concentrations of boron that were just below 150 μg/g and just above 100 μg/g [18, 19].

PHITS is a Monte Carlo-based simulation software capable of modeling particle interactions with energies up to 1TeV. Figure 2 shows the types of calculation models available in PHITS, including *Intranuclear cascade* (INCL 4.6), JEND, ATIMA, and EGS5 for various interactions [20].

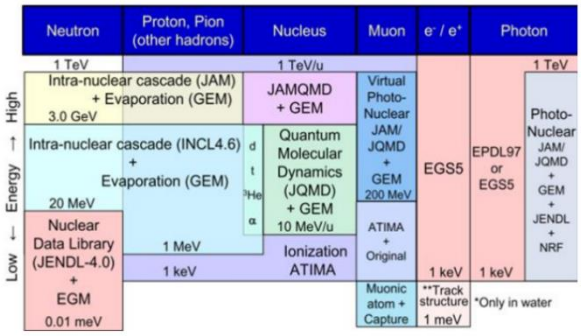

Figure 2. Model physics PHITS [20]

This research focuses on the utilization of the BNCT method for cervical cancer therapy, as well as how boron concentration affects individuals receiving therapy for cervical cancer in terms of dose rate and irradiation duration. Therefore, the dose calculation uses the PHITS version 3.33 program to accumulate the dose calculation so that it will know the irradiation time needed for cancer therapy.

2. METHODOLOGY

This simulation focuses on analyzing boron dosing in cancer treatment, specifically through Boron Neutron Capture Therapy (BNCT), using the PHITS program. PHITS facilitates dose evaluation and visualization of particle trajectories, along with other capabilities, as shown in Figure 2 [15]. Following an extensive review of relevant literature, a detailed case study was undertaken, emphasizing the categorization of the research materials:

2.1 Cervical cancer geometry

This study uses a cancer geometry model based on the *Oak Ridge National Laboratory* (ORNL) phantom, specifically designed for adult Asian females. The model incorporates organ constituent materials derived from the guidelines established by the *International Commission on Radiation Units* (ICRU). A phantom, a computational or physical model of human anatomy, is widely employed in radiology for dose simulation [21]. The mass fraction of body tissue components is critical, as different tissue types respond differently to neutron interactions, resulting in varying radiation dose absorption. Each part of an organ reacts differently when it comes into contact with neutrons, which means the amount of radiation dose the tissue receives can be different. Materials should closely match actual human tissues because their composition affects radiation interactions; consequently, the dose rate [22, 23].

Radiotherapy planning ensures that the target area receives the maximum therapeutic dose while minimizing exposure to healthy tissues. This can be achieved using a computer-based *Treatment Planning System* (TPS) [24]. The TPS outlines key volumetric parameters for radiation therapy. The *Gross Tumor Volume* (GTV) delineates the extent of the tumor that is discernible through imaging modalities and clinical assessments. The Clinical Target Volume (CTV) comprises the GTV along with an added margin to account for potential subclinical disease spread. The *Planning Target Volume* (PTV) expands the CTV with an additional margin for patient positioning uncertainties, improving radiation delivery precision [20]. The cancer structure consists of a layered sphere measuring 3.2 cm in diameter, categorized as stage IIIA. The geometry modeling is based on the FDG PET/CT scan results shown in Fig. 3. FDG PET/CT is a diagnostic imaging modality that combines anatomical and metabolic information, making it highly effective for detecting and staging various cancers and other diseases. It is a very good tool for diagnosing many types of cancer and other diseases. It combines anatomical imaging with functional information about tissue metabolism. This provides more comprehensive diagnostic information than either CT or MRI alone [25].

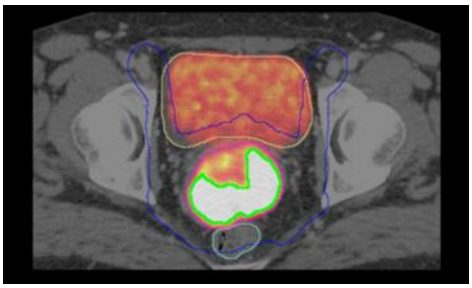

Figure 3. FDG PET/CT scan results of axial section [26]

Utilizing the PHITS program for modeling is essential to enhance the visualization of the phantom, allowing for more accurate analyses and interpretations in research. The results of geometry modeling were carried out using the PHITS program as shown in the following Figure 4.

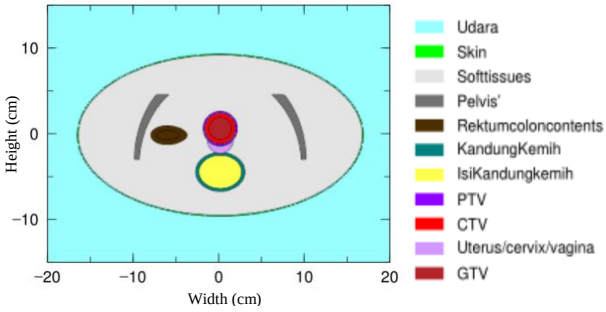

Figure 4. Modeling of ORNL phantom axial cross-section geometry

2.2 Neutron source

Neutron sources are traditionally derived from nuclear reactors; however, inherent limitations make them less suitable for certain applications. In response, accelerator-based BNCT facilities have been developed. In these systems, fast neutrons are generated by proton bombardment of lithium or beryllium targets. To achieve the required thermalization, fast neutrons are moderated using a *Beam Shaping Assembly* (BSA), which shapes and directs the neutron flux for therapeutic purposes [27].

The BSA system is capable of generating a neutron flux appropriate for therapeutic applications due to its incorporation of various components. Central to this process are moderators that facilitate the reduction of fast neutron energies, transitioning them into the thermal or epithermal energy spectrum. Careful selection of materials, such as Aluminum, is essential to ensure the system meets specifications for effective neutron therapy [22, 28, 29]. Shown in Table 5.

Table 2. BSA building blocks [28]

No	Components of BSA	Material
1	Aperture	Ni 95%
2	Delimiter	Lithiated Polyethylene
3	Gamma Shield	Pb
4	Gamma Filter	Bi
5	Neutron Shield	Boroted Paraffin Wax 45%
6	Thermal Neutron Filter	B_4C
7	Fast Neutron Filter	LiF
8	Reflector	PbF^2
9	Moderator	Al
10	Target	Be

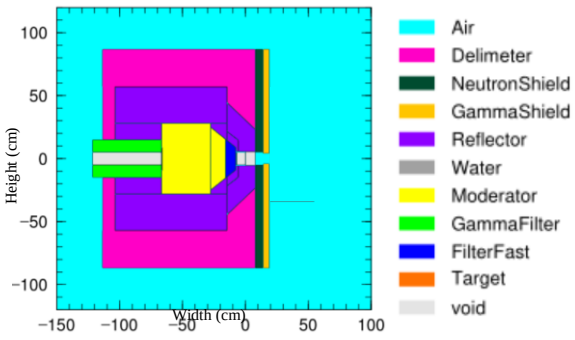

Figure 5. Model beam shaping assembly

The visualization of BSA, generated by the PHITS program, is based on the BSA materials outlined in Table 5 and is illustrated in Figure 5.

Table 3. Parameter IAEA [6]

Parameter	Notes	IAEA Recommendations	Collimator Results
Flux neutron epithermal	$\Phi_{epi}(n.cm^{-2}.s^{-1})$	$> 1.0 \times 10^{9}$	$2.58\ x\ 10^{9}$
Ratio of thermal flux to epitaxial neutron flux	Φ_{th}/Φ_{epi}	< 0.05	$1.73\ x\ 10^{-2}$
Ratio of neutron current to epithermal neutron flux	J/Φ_{epi}	> 0.7	$7.23\ x\ 10^{-1}$
Ratio of fast neutron dose rate to epithermal neutron flux	$\dot{D}_f/\Phi_{epi}\ (Gy.cm^2.n^{-1})$	$< 2.0 \times 10^{-13}$	$5.37\ x\ 10^{-23}$
Ratio of gamma dose rate to epithermal neutron flux	$\dot{D}_\gamma/\Phi_{epi}\ (Gy.cm^2.n^{-1})$	$< 2.0 \times 10^{-13}$	$1.24\ x\ 10^{-22}$

BSA effectively attenuates both fast and thermal neutrons emitted from the radiation source. The filtering methodology is designed to effectively target thermal neutrons, facilitating the production of an epithermal neutron beam that complies with IAEA standards [22]. Table 6 shows the calculation results of the BSA output recommended by the IAEA [30]. The parameters associated with neutron flux values are critical in optimizing therapeutic outcomes for BNCT. The epithermal neutron flux is specifically designed to penetrate biological tissue and target cancerous cells that have taken up boron. It is essential to evaluate the ratio of thermal to epithermal flux, as this metric ensures that the neutrons interacting with the tumor remain within an effective energy spectrum. Furthermore, the neutron current density relative to the epithermal flux should remain high to minimize dispersal: this ratio is crucial for assessing both the distribution and efficacy of neutron delivery to the tumor site. If this value falls below recommended thresholds, achieving adequate neutron interaction with cancerous tissue may become significantly compromised [31, 32].

2.3 Dosage calculation

The radiation field in BNCT comprises four components of radiation, each defined by specific biological weight factors. These four components are [33].

a. Dose of Boron

Eq. 1 shows the dose resulting from thermal neutron reaction with boron-10.

b. Dose of Proton

When thermal neutrons interact with nitrogen-14, they produce carbon-14 and protons, releasing 0.66 MeV of energy. This reaction is a significant source of proton dosage [15].

$$^{14}_{7}N + ^{1}_{0}n\ (0{,}0025\ eV) \rightarrow\ ^{14}_{6}C +\ ^{1}_{1}p\ (0{,}66\ MeV) \quad (2)$$

c. Dose of Gamma

The gamma dose encompasses both the gamma radiation emitted alongside the neutron beam and the gamma rays generated within the biological tissue as a result of neutron interactions [33].

$$^{1}_{1}H + ^{1}_{0}n\ (0{,}0025\ eV) \rightarrow\ ^{2}_{1}D +\ ^{0}_{0}\gamma\ (2{,}33\ MeV) \quad (3)$$

d. Neutron Scattering Dose

This component is generated by fast neutrons emitted from the neutron source [4]. The dose can be calculated as follows:

2.3.1 Determination of The Tissues' Atomic Count

$$\mathrm{N_{i-tissue}} = \frac{\mathrm{N_i(atom)}}{\mathrm{m_{tissue}(kg)}} \quad (4)$$

The value of N_i, can be calculated using Eq. 5 [34].

$$\mathrm{N_i} = \mathrm{n_i N_A} \quad (5)$$

N_i represents the number of moles of element i, determined using Avogadro's number, as shown in Eq. 6.

$$\mathrm{n_i} = \frac{\mathrm{m_i(gram)}}{\mathrm{Ar_i}\left(\frac{\mathrm{gram}}{\mathrm{mol}}\right)} \quad (6)$$

2.3.2 BNCT Dose Rate Calculation

The dose rate is calculated using Equations (7) through (9), and the total dose rate to body organs is calculated in Equation (10).

1) The determination of the dosage rate is conducted utilizing the following equation [6].

$$\dot{\mathrm{D}}_{\mathrm{boron}} = \frac{\Phi \mathrm{N_{B-tissue}} \sigma_{\mathrm{B}} \mathrm{Q}(1.6 \times 10^{-13})\mathrm{J/MeV}}{1\,\frac{\mathrm{J/kg}}{\mathrm{Gy}}} \quad (7)$$

2) Proton energy is produced when thermal neutrons are captured by nitrogen-14, generating carbon-14 and 0.66 MeV protons. The proton dose rate is quantified using Equation 8[6].

$$\dot{\mathrm{D}}_{\mathrm{proton}} = \frac{\Phi \mathrm{N_{N-tissue}} \sigma_{\mathrm{N}} \mathrm{Q}(1.6 \times 10^{-13})\mathrm{J/MeV}}{1\,\frac{\mathrm{J/kg}}{\mathrm{Gy}}} \quad (8)$$

3) Gamma dose rate, calculated by Eq. 8 [6].

$$\dot{\mathrm{D}}_{\gamma} = \Phi \mathrm{N_{H-tissue}} \sigma_{\mathrm{H}} \Delta_{\phi} \quad (9)$$

The overall dose rate represents the dose equivalent, which quantifies the biological effect of absorbing a given amount of radiation energy,

accounting for all contributing components [6]. The total dose in each tissue, weighted by the radiation quality factor, is calculated as [11]

$$\dot{D}_{total} = W_b \times D_b + W_p \times D_p + W_n \times D_n + W_\gamma \times D_\gamma \quad (10)$$

The notation $W_{b/p/n/\gamma}$ represents the corresponding dose quality factor [19].

2.3.3 Calculation of Irradiation Time

Irradiation time is calculated as the ratio of the minimum therapeutic dose to the total BNCT dose rate [6]. Irradiation time is obtained using the following equation [19].

$$T = \frac{D_{min}}{\dot{D}_{total}} \quad (11)$$

2.3.4 Absorption Dose Calculation

The absorbed dose, expressed in Gray (Gy) which is described as the amount of radiation energy (Joule) deposited in tissue per unit mass (Kg) [35]. The absorbed dose is calculated using the following equation:

$$D_{absorbed} = \dot{D}.t_{irradiation} \quad (12)$$

3. RESULTS AND DISCUSSION

This study employed two irradiation directions *left-lateral* and *posterior-anterior*. The simulation angles in PHITS using 270° and 360° as seen in Figure 6 for the direction *posterior-anterior* and Figure 7 for the direction *left-lateral*. The distance between the BSA and the ORNL phantom was set to 0.2 cm, representing the closest distance from the BSA output. Two irradiation directions were selected to minimize the dose received by the *Organ at Risk* (OAR) and reduce side effects.

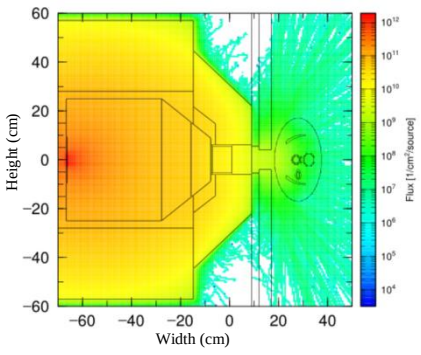

Figure 6. *Posterior-anterior* irradiation direction

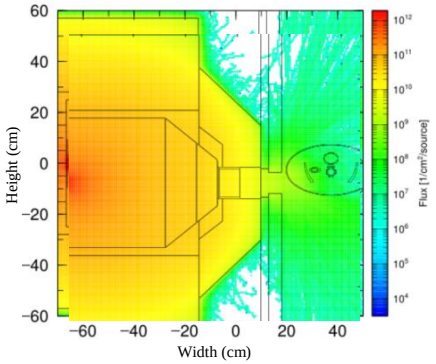

Figure 7. *Left-lateral* irradiation direction

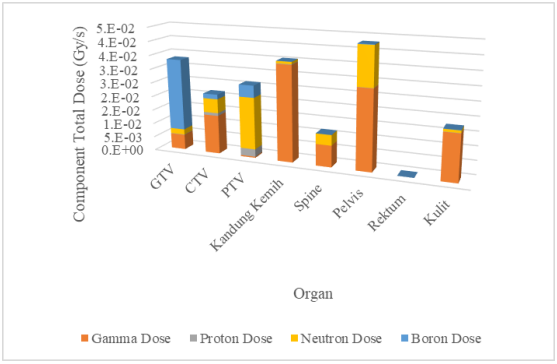

Figure. 8. Components of dose rate at a concentration of 140 µg/g from the *left-lateral* direction

The components of the dose received in each organ for a boron concentration of 140 µg/g in the *left-lateral* direction are shown in Figure 8. Among the four dose components, the boron dose in the GTV is the highest on average. This graph is important for treatment planning and understanding radiation exposure in patients. In BNCT, the enhanced dose rate of boron observed in the GTV can be attributed to the significantly higher concentration of Boron-10 within the cancerous tissue compared to that in OAR. This is expected, as alpha particles are the primary radiation modality for tumor ionization in BNCT.

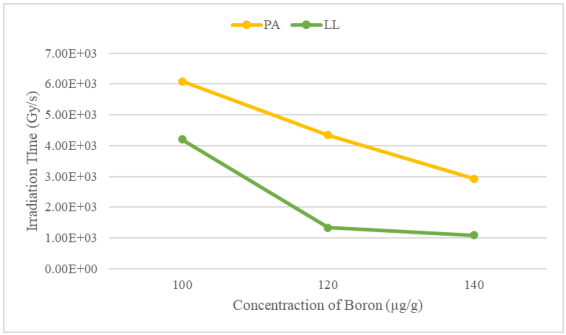

Figure 9. Irradiation time of 2 irradiation directions

Figure 9 shows the relationship between irradiation time and boron concentration for the two irradiation directions. Irradiation duration is determined by dividing the required therapeutic dose for effective cancer cell ablation by the cumulative BNCT dose rate, as shown in Eq. 11. Since the GTV represents the primary tumor volume, the total dose rate was based on the GTV section. The threshold dose required to effectively eradicate cervical cancer cells is 95 Gy [26]. Irradiation time was calculated by dividing the minimum required dose by the overall dose rate at the GTV. Based on simulation results, *posterior-anterior* irradiation produced treatment times of 101, 72, and 48 minutes for boron concentrations of 100, 120, and 140 µg/g, respectively. *Left-lateral* irradiation resulted in times were 69, 22, and 18 minutes for the same concentration.

Figure 9 shows that when the concentration of boron-10 increases, the resulting irradiation duration decreases. The longest treatment time, 101 minutes 42 seconds, occurred at a ureboron concentration of 100 µg/g in the *posterior-anterior* direction, while the shortest time, 18 minutes 22 seconds, was achieved at 140 µg/g in the *left-lateral* direction, corresponding to a total dose rate of $8.69\text{x}10^{-2}$ Gy/s.

Table 4. Dose rate and irradiation time at 2 irradiation directions

Concentration (µg/g)	Left-lateral		Posterior- Anterior	
	Total Dose Rate (Gy/s)	Irradiation Time (minutes)	Total Dose Rate (Gy/s)	Irradiation Time (minutes)
100	$2.27\text{x}10^{-2}$	69	$1.56\text{x}10^{-2}$	101
120	$7.14\text{x}10^{-2}$	22	$2.19\text{x}10^{-2}$	72
140	$8.69\text{x}10^{-2}$	18	$3.25\text{x}10^{-2}$	48

The results of the total dose calculation are thoroughly presented in Table 7, which includes a comparative analysis of dose rates and irradiation times across various boron concentrations. The data clearly indicate that the *left-lateral* irradiation direction consistently requires less time for irradiation than the *posterior-anterior* direction across all tested boron concentrations. This difference can be ascribed to the comparatively higher dose rate observed in the left-lateral orientation, recorded at $8.69\text{x}10^{-2}$ Gy/s, in contrast to the lower dose rate measured in the posterior-anterior direction, which stands at $3.25\text{x}10^{-2}$ Gy/s. This aligns with the findings of Pramusinta *et al. (2019)*, which indicate that the total dose delivered to cancerous tissues correlates positively with the concentration of boron. In summary, an increase in systemically delivered boron concentration correlates with greater absorption by tumor tissues, thereby enhancing the therapeutic efficacy against malignant cells [36].

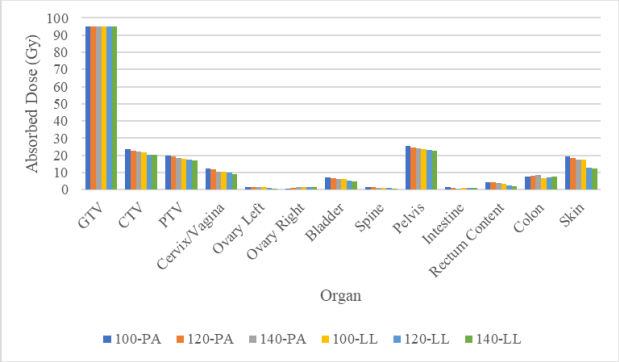

Figure 10. Absorbed dose in each tissue

As shown in Figure 10, the absorbed dose values for each tissue across different irradiation directions and boron concentrations are presented in a bar chart. The absorbed dose value in GTV tissue reaches 95 Gy, which represents the minimum threshold considered sufficient for the eradiction of cancerous cells. The absorbed dose to healthy tissue diminishes as the boron concentration increases, owing to the higher dose rate that shortens the irradiation time. This reduction in exposure duration limits the OAR from receiving prolonged high radiation levels. These results are consistent with findings from Bilalodin *et al*. (2023), who reported that higher boron concentrations increase dose rates, thereby influencing both irradiation time and the dose absorption by OAR [6].

The absorbed dose to healthy skin tissue remains below the permissible threshold for normal cells (14.4 Gy) [37]. At this threshold, the most likely side effect is desquamation-characterized by the shedding of epithelial layers as scales or fine sheets [38]. For the rectum and bladder, the highest absorbed doses were 4.4 Gy and 7.2 Gy, respectively, both recorded at a boron concentration of 100 µg/g from the *posterior-anterior* direction.

4. CONCLUSION

The PHITS code was employed to calculate dose components in cervical cancer treatment using BNCT, with a Beam Shaping Assembly (BSA) serving as the neutron source. The simulation's findings demonstrate that increasing boron concentration shortens irradiation time by increasing the dose rate to the tumor.

For GTV tissue, the dose rate values at 100, 120, and 140 μg/g from the *posterior-anterior* direction for GTV tissue were 0.015611 Gy/s, 0.021911 Gy/s, and 0.032513 Gy/s, and for the *left-lateral* direction, the corresponding values were 0.022635 Gy/s, 0.071434 Gy/s, and 0.086885 Gy/s. These data confirm that higher boron concentrations result in higher tumor dose rates. A higher dose rate correlates with reduced irradiation time, thereby shortening the overall therapeutic duration.

The highst dose rate- 8.68×10^{-2} Gy/s was achieved at a boron concentration of 140 μg/g with irradiation from the left-lateral direction. Under these conditions, the estimated treatment time was approximately 18 minutes 22 seconds. This underscores the efficiency of the *left-lateral* approach in delivering the prescribed dose, offering potential advantages for treatment planning and clinical applications.

Overall, these findings emphasize the importance of optimizing both boron concentration and irradiation duration in cervical cancer BNCT. By enabling a more targeted approach, the proposed parameters have the potential to reduce adverse side effects while improving therapeutic efficacy. Moreover, this study contributes to a deeper understanding of the underlying biological mechanisms, which may guide the development of more effective and patient-friendly treatment strategies in the future.

ACKNOWLEDGMENTS

This research could not have been completed without the invaluable contributions and support from numerous individuals and organizations. Accordingly, the author wishes to express sincere gratitude to the following parties:

1. The Indonesian Ministry of Education, Culture, Research, and Technology collaborates with the Center for Research on Nuclear Technology, Safety, Metrology, and Quality (PRTKMMN) and the National Research and Innovation Agency (BRIN), and Oversees the Merdeka Belajar Kampus Merdeka (MBKM) internship program. This initiative aims to enhance practical learning experiences by integrating advanced research and technological competencies within higher education frameworks, fostering a culture of innovation and interdisciplinary collaboration.
2. The backing from the Ministry of Religious Affairs facilitated the seamless execution and overall success of the research project.
3. The UIN Sultan Maulana Hasanuddin Banten has significantly contributed to this research project by offering valuable insights and guidance throughout the process.

AUTHOR CONTRIBUTIONS

Laili Rochimah: Ideas, formulation or evolution of overarching research goals and aims, oversight and leadership responsibility for the research activity planning and execution, including mentorship external to the core team cancer therapy, management and coordination responsibility for the research activity planning and execution, **Subur Pramono:** Development or design of methodology, creation of models, **Beta Nur Pratiwi:** Programming, software development, designing computer programs, implementation of the computer PHITS code and supporting algorithms, testing of existing PHITS code components, **Yohannes Sardjono:** Verification, whether as a part of the activity or separate, of the overall replication/ reproducibility of results/experiments and other research outputs, **Gede Sutesna Wijaya:** Application of statistical, mathematical, computational, or other formal techniques to analyze or synthesize study data, **Isman Mulyadi Triatmoko:** Conducting a research and investigation process, specifically performing the experiments, or data/evidence collection, **Nunung Nuraeni:** Provision of study materials, reagents, materials, patients, laboratory samples, animals, instrumentation, computing resources, or other analysis tools, **Heru Prasetio:** Management activities to annotate (produce metadata), scrub data

and maintain research data (including software PHITS code, where it is necessary for interpreting the data itself) for initial use and later reuse, **Nur Rahmah Hidayati:** Preparation, creation and/or presentation of the published work, specifically writing the initial draft (including substantive translation), **Syarifatul Ulya:** Preparation, creation and/or presentation of the published work by those from the original research group, specifically critical review, commentary or revision – including pre-or postpublication stages and **Zuhdi Ismail:** Preparation, creation and/or presentation of the published work, specifically visualization/ data presentation are the main contributors to this writing. All authors have read and approved the final version of this paper.

NOMENCLATURE

Φ_{epi}	=	Flux epithermal
Φ_{th}	=	Flux thermal
$N_{i\text{-}tissue}$	=	Number of atoms of element *i* (atom/ kg tissues)
N_i	=	Number of atoms
m_{tissue}	=	Mass of the tissue (kg)
N_A	=	Avogadro number (6.023 x 10^{23}atom/mol)
n_i	=	Mole of element *i* (mol)
m_i	=	Massa of element *i* (g)
Ar_i	=	Number mass of element *i* (g/mol)
$\dot{D}_{boron}$	=	Dose rate of boron (Gy/s)
$\dot{D}_{proton}$	=	Dose rate of proton (Gy/s)
$\dot{D}_{\gamma}$	=	Dose rate of gamma (Gy/s)
Φ	=	Fluent neutron thermal ($n.cm^{-2}.s^{-1}$)
$N_{B\text{-}tissue}$	=	Amount of boron (atom/kg)
$N_{N\text{-}tissue}$	=	Amount of nitrogen (atom/kg)
$N_{H\text{-}tissue}$	=	Amount of hydrogen (atom/kg)
σ	=	Cross section (cm^2)
Q	=	Particle energy (MeV)
Δ_{ϕ}	=	Coefficient of dose rate
$\dot{D}_{total}$	=	Dose rate total (Gy/s)
w_b	=	Quality factor boron
w_p	=	Quality factor proton
w_n	=	Quality factor neutron
w_{γ}	=	Quality factor gamma
D_{total}	=	Dose total
D_{min}	=	Dose minimum (Gy)
$\dot{D}_{absorbed}$	=	Absorbed dose value (Gy)
$\dot{D}$	=	Dose rate value (Gy/s)
$T/t_{irradiation}$	=	Irradiation time (s)

REFERENCES

1. Zhang S., Xu H., Zhang L., Qiao Y. Cervical Cancer: Epidemiology, Risk Factors and Screening. Chinese J. Cancer Res. 2020. **32**(6):720–8.
2. Novalia V. Kanker Serviks. Galen. J. Kedokt. dan Kesehat. Mhs. Malikussaleh. 2023. **2**(1):45.
3. Agus Permana G.P., Sardjono Y., Widodo S. Boron Analysis and Imaging in Boron Neutron Capture Therapy (BNCT). Indones. J. Phys. Nucl. Appl. 2020. **5**:38–60.
4. Jalut L.L.S., Rupiasih N.N., Sardjono Y. Analysis Dosage of Boron in BNCT with Simulation Method Using PHITS (Particle and Heavy Ion Transport Code System) Program. Bul. Fis. 2020. **21**(1):1–7.
5. Dai Q., Yang Q., Bao X., Chen J., Han M., Wei Q. The Development of Boron Analysis and Imaging in Boron Neutron Capture Therapy (BNCT). Mol. Pharm. 2022. **19**(2):363–77.
6. Bilalodin B., Wihantoro, Haryadi A., Abdullatif F. Dosimetry Analysis of Boron Neutron Capture Therapy (BNCT) on Thyroid Cancer using PHITS Code with Neutron from 30 MeV Cyclotron. J. Teknol. 2023. **85**(5):21–6.
7. Suzuki M. Boron Neutron Capture Therapy (BNCT): A Unique Role in Radiotherapy with a View to Entering the Accelerator-based BNCT Era. Int. J. Clin. Oncol. 2020. **25**(1):43–50.
8. Ardana I.M., Noerwasana A.D., Sardjono Y. *Kajian Teknologi Boron Neutron Capture Therapy (BNCT) dan Aspek regulasinya*. Research Gate. 2021.
9. JAEA *Nuclear Data Center* [Accessed: 1 September 2024]. Available from: https://wwwndc.jaea.go.jp/jendl/j40/j40nat.html.
10. Dymova M.A., Taskaev S.Y., Kuligina E.V. Boron Neutron Capture Therapy : Current Status and Future Perspectives. John Wiley Sons Aust. 2020. **40**:406–21.
11. Mbagwu J. Theoretical Investigation of Dosimeter Accuracy for Linear Energy Transfer Measurements in Proton Therapy : A Comparative Study of Stopping Power Ratios. Radiat. Phys. Chem. 2025. **227**:112354.
12. Kalholm F., Grzanka L., Traneus E., Bassler N. A Systematic Review on the Usage of Averaged LET in Radiation Biology for Particle Therapy. Radiother. Oncol. 2021. **161**:211–21.
13. Lestari F., Hasbiyah, Hardiana S., Ramdani R. Numerical Analysis of Fussion Cross Section of 12C + 12C and 16O + 58,60,64 Ni System Using The Modifid Glas-Mosel Formula. J. Apl. Fis. 2024. **20**(2):9–16.
14. Hosch W.L. *Cross Section* [Accessed: 14 January 2025]. Available from: https://www.britannica.com/science/cross-section-physics.
15. Chino Y., Senoo Y., Chiel H.J., Thomas P.J., Design M., Escalona-villalpando R.A., et al. Dose analysis of Boron Neutron Capture Therapy (BNCT) on head cancer using PHITS code with neutron source from accelerator. J. Phys. Conf. Ser. 2022.:1–7.

16. Yani S., Hadijah S., Husin D., Fisika D., Matematika F., Alam P., et al. Analisis Parameter Keluaran pada Kolom Termal Reaktor Kartini untuk Boron Neutron Capture Therapy (BNCT) dengan Software Phits. J. Fis. 2022. **12**(2):55–64.
17. Puspita R.. *Analisis Dosis Radiasi Terapi Kanker Serviks Dengan Boron Neutron Capture Therapy (BNCT) Berbasis Particle and Heavy Ion Transport code System (PHITS)*.Universitas Gadjah Mada; 2021.
18. Agestha M. *Perhitungan Dosis Pada Terapi Kanker Serviks Dengan Metode Boron Neutron Capture Therapy (BNCT) Melalui Pemanfaatan PHITS 3.26*.Universitas Gadjah Mada; 2023.
19. Bilalodin, Haryadi A., Abdullatif F. Dose Analysis of Boron Neutron Capture Therapy (BNCT) on Head Cancer using PHITS Code with Neutron Source from Accelerator. in: *Journal of Physics: Conference Series*. 2023.
20. Mutamimah R., Sardjono Y. Aplikasi Program PHITS Versi 3.21 untuk Analisis Dosis Radiasi Pada Terapi Kanker Otak dengan Metode Proton Therapy. Unnes Phys. Educ. J. 2022. **11**(1):26–35.
21. Puspitasari R.A., Pertiwi W.I., Maratus Sholihah P., Fariqoh W.H., Kavilani N., Dyah S., et al. Analisis Kualitas Berkas Radiasi LINAC Untuk Effektivitas Radioterapi. J. Biosains Pascasarj. 2020. **22**(1):11–9.
22. Pratiwi A. *Dose Analysis of Boron Neutron Capture Therapy (BNCT) for Ovarian Cancer Metastasis Treatment Using PHITS 3.26*. Universitas Gadjah Mada; 2022.
23. Nurfatthan I. A*nalisis Dosis dan Waktu Terapi pada Terapi Kanker Paru-paru Berbasis Terapi Ion Karbon dan Boron Neutron Capture therapy menggunakan program PHITS*.Universitas Gadjah Mada; 2019.
24. Farhiyati W., Subroto R., Makmur I.W.A., Qomariyah N., Wirawan R. Treatment Planning System (Tps) Kanker Payudara Menggunakan Teknik 3DCRT. ORBITA J. Kajian, Inov. dan Apl. Pendidik. Fis. 2020. **6**(1):150.
25. Singnurkar A., Poon R., Metser U., Ct P.E.T., Mri P.E.T. Head-to-Head Comparison of the Diagnostic Performance of FDG PET / CT and FDG PET / MRI in Patients With Cancer : A Systematic Review and Meta-Analysis. Am. J. Roentgenol. 2024.(September)
26. Arnesen M.R., Rekstad B.L., Stokke C., Bruheim K., Løndalen A.M., Hellebust T.P., et al. Short-course PET-based Simultaneous Integrated Boost for locally advanced cervical cancer. Radiat. Oncol. 2016. **11**:1–8.
27. Li G., Jiang W., Zhang L., Chen W., Li Q. Design of Beam Shaping Assemblies for Accelerator-Based BNCT With. 2021. **9**(March):1–10.
28. Ardana I.M., Kusminarto K., Sardjono Y. Optimization of a Beam Shaping Assembly Design for Boron Neutron Capture Cancer Therapy Facility Based on 30 MeV Cyclotron. Indones. J. Phys. Nucl. Appl. 2016. **1**(3):128.
29. Soedirman U.J. Tinjauan Umum Boron Neutron Capture Therapy (BNCT) sebagai Metode Terapi Kanker. 2023.
30. Richter L.E., Carlos A., Beber D.M. Advances in Boron Neutron Capture Therapy. 2023.
31. Sánchez P.T., Porras I., Chernenko N.R., Saavedra F.A. De, Praena J. *Optimized Beam Shaping Assembly for a 2 . 1 - MeV Proton - Accelerator - based Neutron Source for Boron Neutron Capture Therapy*. Scientific Reports.Nature Publishing Group UK; 2021.
32. Nobakht E., Fouladi N. Feasibility Study on the Use of 230 MeV Proton Cyclotron in Proton Therapy Centers as a Spallation Neutron Source for BNCT. Reports Pract. Oncol. Radiother. 2019. **24**(6):644–53.
33. Hu N., Tanaka H., Takata T., Endo S., Masunaga S., Suzuki M., et al. Evaluation of PHITS for Microdosimetry in BNCT to Support Radiobiological Research. 2020. **161** (November 2019)
34. Nishitani T., Yoshihashi S., Tanagami Y., Tsuchida K., Honda S., Yamazaki A., et al. Neutronics Analyses of the Radiation Field at the Accelerator-Based Neutron Source of Nagoya University for the BNCT Study. J. Nucl. Eng. 2022. **3**(3):222–32.
35. ICRP *Adult Mesh-type Reference Computational Phantoms*.Sage, 2019.
36. Pramusinta R., Pramusinta R., Zailani R., Sardjono Y. Dose Analysis in Boron Neutron-capture Cancer Therapy (BNCT) Neutron Generator Based on Breast Cancer. Indones. J. Phys. Nucl. Appl. 2019. **4**(1):8–11.
37. Coia L., Emami B., Solin L.J., Munzenrider J.E., Lyman J., Shank B., et al. *Tolerance of Normal Tissue to Therapeutic Radiation*. Springer. 2013.
38. Miller C., Crampin E., Osborne J. Multiscale Modelling of Desquamation in the Interfollicular Epidermis. PLOS Comput. Biol. 2022.:1–33.

This page is intentionally blank